Journal of Chemical&Engineering Data

pubs.acs.org/jced Article

Molecular Interactions Studies of Dimethyl Sulfoxide, *N*-Methyl-2-pyrrolidone, and Water Binary Mixtures at Varying Temperatures: Volumetric and Spectroscopic Investigations

Published as part of Journal of Chemical & Engineering Data special issue "ICTAC 2024".

Praseeda P. Nair, Aditi Prabhune, Sanjay Kumar, and Ranjan Dey*

Cite This: https://doi.org/10.1021/acs.jced.5c00049 Read Online

ACCESS | Metrics & More | Article Recommendations | Supporting Information

ABSTRACT: Thermophysical properties are crucial for various industrial applications, process designs, and modeling as they provide insight into intermolecular interactions. In this work, the binary mixtures of polar aprotic solvents dimethyl sulfoxide (DMSO) and *N*-methyl-2-pyrrolidone (NMP) with a polar protic solvent, water, has been investigated to assess intermolecular interactions and structural behavior. Density (ρ), molar volume (V_m), and coefficient of thermal expansion (α_p) along with excess coefficient of thermal expansion (α_p^E), excess molar volume (V_m^E), and FTIR analysis of binary mixtures were evaluated at various temperatures (293.15−318.15 K). The result reveals that a strong hydrogen-bonding network of water molecules is broken down by DMSO and NMP molecules between 0.3 and 0.4 mole fractions. The new network of hydrogen bonding formed within DMSO + water and NMP + water is strong and hetero-associated, expressed by the negative value of V_m^E. The packing factor in NMP + water affects V_m^E showing more molecular interactions than DMSO + water. The DMSO + NMP mixture reveals positive V_m^E values, indicating the self-association of polar solvents.

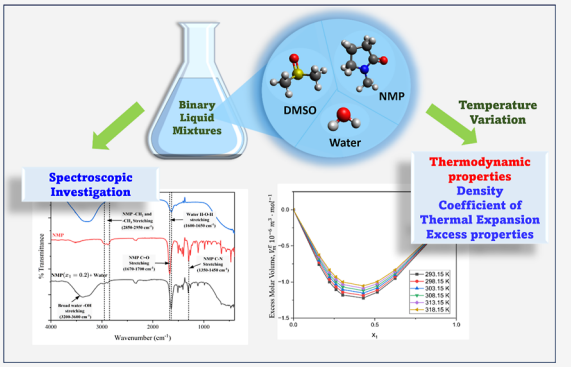

1. INTRODUCTION

The study of solvents and solutions is of significant scientific and industrial importance.[1] Solvation behavior encompasses a variety of intermolecular interactions, including van der Waals forces, ionic/dipolar interactions, hydrogen bonding, and charge transfer. Solvents, which act as reaction media, play a crucial role in influencing both the thermodynamic and kinetic aspects of chemical and physical processes.[2] Most industrial solvents are extensively employed across diverse industries for applications such as surface preparation, cleaning, and serving as reaction media in adhesive manufacturing, biotechnology,[3] and shipbuilding.[4] Although sustained efforts are on globally[5] to minimize the usage of these commercial solvents due to their environmental and health concerns as most of these solvents are Volatile Organic Compounds (VOCs)[6] which are carcinogenic, mutagenic, and teratogenic in nature,[7] they remain indispensable for achieving desired product properties and process efficiencies due to the lack of more benign greener and sustainable alternatives.[8]

Polar aprotic solvents are widely utilized on both laboratory and industrial scales due to their versatility and ability to dissolve a broad range of solutes.[9] Their applications span multiple fields, including chemistry, biochemistry, nanoscience, and pharmaceuticals.[10] Among polar aprotic solvents, dimethyl sulfoxide (DMSO) and *N*-methyl-2-pyrrolidone (NMP) are especially noteworthy. Their mixture with water, a polar protic solvent, may have produced distinct molecular interactions. Along with the chemical nature of components, the size and structure of the molecules as represented in Figure 1 contribute to molecular behavior when mixed.

DMSO, a byproduct of the wood industry, is widely recognized for its utility in organic synthesis and pharmaceutical processes due to its low cost, excellent stability, and high solvating power.[11] NMP, a petroleum-derived solvent, is another highly effective solubilizing agent[12] with diverse industrial applications, including petrochemical processing, battery manufacturing,[13] production of agricultural chemicals, and industrial cleaning.[14] The unique physicochemical properties of these solvents make them critical in various industrial operations.

Received: January 27, 2025
Revised: June 5, 2025
Accepted: June 13, 2025

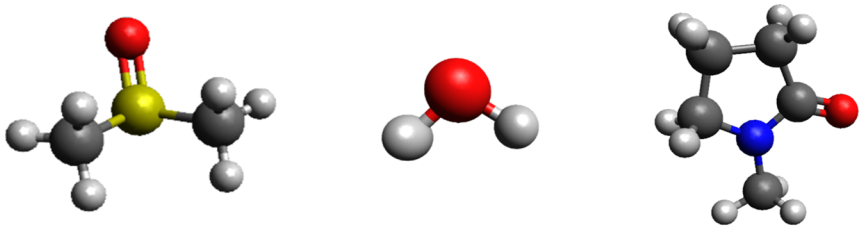

(a) (b) (c)

Figure 1. Molecules of (a) DMSO, (b) water, and (c) NMP.

Thermophysical properties, such as density, viscosity, ultrasonic velocity, and refractive index, provide essential insights into molecular interactions and mixture behavior. These properties are fundamental for the design and optimization of numerous industrial processes, including heat and mass transfer, fluid flow, separation processes, and wastewater treatment systems.[15−17] Density[18] provides fundamental information about molecular packing and interactions within mixtures, which is crucial for the design of separation processes and fluid flow systems. The excess coefficient of thermal expansion,[19] on the other hand, reveals how volumetric changes respond to temperature variations, offering critical insights into the thermal stability and compatibility of mixtures under varying industrial conditions. Additionally, understanding thermophysical properties aids in developing theoretical models, designing novel materials, optimizing energy systems, and ensuring both environmental and operational safety.[20]

The investigation of DMSO−water, NMP−water, and DMSO−NMP binary mixtures is therefore of significant interest. Such studies not only enhance our understanding of intermolecular interactions but also contribute to improving industrial processes, particularly those involving solvent mixtures in sustainable and energy-efficient systems.

2. EXPERIMENTAL METHODS

Dimethyl sulfoxide and *N*-methyl-2-pyrrolidone have been supplied by LOBA Chemie Pvt., Ltd. and used without further purification. More details about the chemicals are mentioned in Table 1. Pure distilled water was utilized for the preparation of binary liquid mixtures. The mixtures were prepared by mass, and weighing was done using a Shimadzu Uni Bloc AP225WD balance with precision ±0.0001 g. The uncertainty in mole fraction was estimated to be $\pm 1 \times 10^{-4}$. The density of pure liquids and mixtures was measured using a densimeter (Rudolph DDM 2911) with an accuracy of ±0.05 kg·m^{-3}. The instrument was calibrated at 293.15 K using the air and water calibration method before the measurement of the liquid sample and thoroughly cleaned before and after measurement with pure distilled water and acetone. Densities of the pure liquids have been compared with literature data, as presented in Table 2 to ascertain the consistency. The standard uncertainty for the density measurement is ±0.05 kg·m^{-3}. The estimated standard uncertainties of V_m^E and α_P are $\pm 0.005 \times 10^{-6}$m^3·mol^{-1} and $\pm 0.05 \times 10^{-4}$ K^{-1}, respectively.

Table 1. List of Chemicals with Details of Source, CAS Number, and Mass Fraction Purity

chemical	source	CAS number	molar mass	mass fraction purity
dimethyl sulfoxide	LOBA Chemie Pvt., Ltd.	67-68-5	78.13	>0.99
N-methyl-2-pyrrolidone	LOBA Chemie Pvt., Ltd.	872-50-4	99.13	>0.98

Fourier-transform infrared (FTIR) spectroscopy using the ATR technique was performed for selected binary mixtures to investigate the intermolecular interactions and confirm the presence of functional groups. The analysis was carried out using a Shimadzu IR Affinity-1 instrument at 298.15 K. Samples of the binary mixtures with lower and higher concentrations of x_1 were used for the study. A small amount of each mixture was placed on the instrument's sample holder, and spectra were recorded over the wavenumber range of 4000−400 cm^{-1}. The FTIR spectra were analyzed to identify specific vibrational modes associated with molecular interactions, such as hydrogen bonding and dipole−dipole interactions, providing deeper insights into the structural and dynamic behavior of the mixtures.

3. RESULTS AND DISCUSSION

The densities (ρ) have been determined experimentally at the temperatures 293.15−318.15 K and atmospheric pressure, for pure components and binary liquid mixtures of dimethyl sulfoxide (DMSO) with water, *N*-methyl-2-pyrrolidone (NMP) with water, and DMSO with NMP. Previously, densities of pure components have been reported by several researchers in the literature.[21,25−31,33−36] The graphical depiction of relative percentage deviations from literature data is given in the Supporting Information (Figures S1−S3). The relative percentage deviation shows good agreement between the literature and experimental values. Also, previously reported density values of similar binary liquid mixtures are compared and graphically represented in the Supporting Information (Figures S4−S6). The graphs show a similar trend in the density variation, and deviations are also observed to be within error measurement, confirming the quality of measurement and the purity of components.

Other derived thermodynamic properties like the molar volume (V_m) and coefficient of thermal expansion (α_P) along with excess properties like excess coefficient of thermal expansion (α_P^E) and excess molar volume (V_m^E) have been evaluated for the same binary liquid mixtures at various temperatures. The density (ρ) of mixtures and pure components has been utilized to calculate excess molar volume using the expression[37]

https://doi.org/10.1021/acs.jced.5c00049
J. Chem. Eng. Data XXXX, XXX, XXX−XXX

Table 2. Densities, ρ, of Pure Liquid Components at Different Temperatures, T/K = (293.15−318.15) and Pressure, p = 0.1 MPa[a]

	ρ (kg·m^{-3})					
	water		DMSO		NMP	
T/K	exp. (this work)	literature	exp. (this work)	literature	exp. (this work)	literature
293.15	998.21	998.207,[21] 998.20,[22] 998.23[23]	1100.31	1100.3,[24] 1100.2,[25] 1100.41,[22] 1100.76[26]	1032.37	1030.4,[27] 1032.313[28]
298.15	997.04	997.047,[21] 997.05[29]	1095.26	1095.19,[25] 1095.36,[30] 1095.74[26]	1027.88	1028.2,[31] 1028.1,[32] 1028.31,[33] 1025.9,[27] 1027.962[28]
303.15	995.63	995.649,[21] 995.64,[22] 995.65,[29] 995.68[23]	1090.24	1090.18,[25] 1090.37[22], 1090.34[30], 1090.73[26]	1023.43	1021.71,[27] 1023.521[28]
308.15	994.01	994.033,[21] 994.03[29]	1085.22	1085.18,[25] 1085.31[30]	1018.97	1019.3,[31] 1019.14,[32] 1019.32,[33] 1015.9,[27] 1019.06[28]
313.15	992.20	992.215,[21] 992.21,[22] 992.22,[29] 992.23[23]	1080.21	1080.4,[24] 1080.17,[25] 1080.34,[22] 1080.29,[30] 1080.69[26]	1014.51	1012.0,[27] 1014.607[28]
318.15	990.17	990.21,[a,21] 990.21[29]	1075.21	1075.15,[25] 1075.27[30]	1010.07	1010.6,[31] 1010.10,[33] 1008.2,[27] 1010.141[28]

[a]Standard uncertainties $u(\rho)$ = 0.001 kg·m^{-3}, $u(T)$ = 0.5 K, $u(p)$ = 10 kPa.

$$V_m^E = \frac{M_1x_1 + M_2x_2}{\rho} - \left(\frac{M_1x_1}{\rho_1} + \frac{M_2x_2}{\rho_2}\right) \quad (1)$$

The coefficient of thermal expansion (α_P) is defined as the relative change in the volume with the temperature under isobaric conditions and is calculated using the density of liquid mixtures by making use of the expression[19]

$$\alpha_P = \frac{1}{V}\left(\frac{\partial V}{\partial T}\right)_P = -\frac{1}{\rho}\left(\frac{\partial \rho}{\partial T}\right)_P \quad (2)$$

The excess counterpart of the coefficient of thermal expansion (α_P^E) is evaluated as[38,39]

$$\alpha_P^E = \alpha_P - \alpha^{id} \text{ where } \alpha^{id} = \phi_1\alpha_{P,1} + \phi_2\alpha_{P,2} \quad (3)$$

and $\phi_1$and ϕ_2 are the volume fractions and are evaluated by $\phi_i = \frac{x_iV_i}{\sum_{i=1}^{j} x_iV_i}$ where V_i is the molar volume of the pure ith component. All of the other symbols have their usual meaning.

The evaluated properties have been listed in Tables 3, 4, and 5.

3.1. DMSO + Water Binary Mixtures. From Table 3, it is evident that for the binary mixtures of DMSO + water, the density of the mixture increases as x_1, the mole fraction of DMSO, increases at all temperatures (293.15 to 318.15 K). Additionally, the density of the mixture decreases gradually with an increase in temperature. The measurement of density of DMSO and water at 293.15 to 318.15 K is compared with the literature[29,35,40] and found results were coincident with the reported values, within experimental error. The coefficient of thermal expansion (α_P) for DMSO + water mixtures shows a positive correlation with both the concentration of DMSO and rising temperatures. This indicates that the thermal response of the mixture becomes more pronounced as the proportion of DMSO increases. The excess molar volume (V_m^E) is graphically represented in Figure 2. It is observed that V_m^E exhibits extrema within the mole fraction range of 0.3 to 0.4 for DMSO in the binary mixture. This behavior highlights the intricate nature of molecular interactions within the mixture. Researchers[29,35,40] have reported a strong affinity between DMSO and water molecules in previous studies reflecting in density and excess molar volume values. The study reveals that the increased concentration of DMSO increases the density of the solution and the most negative value of V_m^E is observed between 0.3 and 0.4 mole fractions. This signifies the presence of strong intermolecular interaction along with molecular packing within the solution which produces the observed negative trend in V_m^E values, which resembles the trend reported in the literature.[29,35,40] The positive value of α_P^E (Figure 3) also aids in the presence of strong intermolecular interactions between DMSO and water molecules.

The strong intermolecular interactions in the DMSO + water liquid mixture are governed by the physical and chemical properties of the individual components. DMSO, an aprotic and highly polar solvent with a pyramidal molecular structure, has a highly polar S═O bond, contributing to its high dielectric constant and dipole moment (3.96 D).[41,42] Water, also a polar solvent, forms an extensive hydrogen-bonding network within its pure state. The addition of DMSO disrupts this network, forming hydrogen bonds with water molecules via the oxygen atom of DMSO.[43]

As the concentration of DMSO increases, a robust hydrogen-bonding network develops within the solution. The literature[41,44] reveals that the hydrogen bond strength between DMSO and water is approximately 0.33 times that of hydrogen bonds between water molecules. Molecular dynamics studies[23] showed that the presence of water in DMSO causes elongation of the S═O bond and contraction of the methyl C−H bonds. FTIR[43] spectroscopy and theoretical calculations can be utilized to confirm the donor/acceptor relationship between DMSO and water molecules. FTIR has been carried out at two different mole fractions of DMSO (x_1 = 0.2 and 0.7) to understand the gradual effect of concentration on intermolecular behavior and compare with the FTIR spectra of pure DMSO and water.

In Figure 4a, DMSO has a lower concentration (x_1 = 0.2) and water has a higher concentration (x_2 = 0.8) in the solution. The band that appeared at 1008.77 cm^{-1} shows a narrowing of the peak and a minor shift in the peak indicative of interactions between DMSO and water (S═O and H−O−H). The H−O−H bending vibration peak broadening at 1650 cm^{-1} confirms the involvement of water in interaction with DMSO. The broadening and shift of O−H stretching vibration of water in a DMSO−water mixture between 3200 and 3650 cm^{-1} is an indication of interaction with DMSO S═O due to H-bonding. As the concentration of DMSO increased from 0.2

https://doi.org/10.1021/acs.jced.5c00049
J. Chem. Eng. Data XXXX, XXX, XXX−XXX

Table 3. Density (ρ), Excess Molar Volume (V_m^E), Coefficient of Thermal Expansion (α_p), and Excess of Coefficient of Thermal Expansion (α_p^E) as a Function of the Mole Fraction of DMSO (x_1) at the Temperatures, T/K = (293.15−318.15) and Pressure, p = 0.1 MPa[a]

DMSO (1) + water (2)				
x_1	ρ (kg·m^{-3})	V_m^E (10^{-6} m^3·mol^{-1})	α_p (10^{-4} K^{-1})	α_p^E (10^{-6} K^{-1})
		293.15 K		
0.0000	998.21	0.0000	3.23	0.00
0.0416	1020.00	−0.1369	4.14	5.32
0.0576	1027.00	−0.1848	4.47	9.80
0.0969	1043.99	−0.3435	5.32	33.89
0.1390	1059.01	−0.5072	6.06	54.76
0.2018	1075.68	−0.7094	6.74	57.68
0.2844	1090.27	−0.9045	7.54	72.06
0.3649	1097.76	−0.9792	7.91	59.79
0.5110	1102.97	−0.9257	8.32	35.19
0.6791	1103.25	−0.6799	8.65	16.13
1.0000	1100.31	0.0000	9.12	0.00
		298.15 K		
0.0000	997.04	0.0000	3.23	0.00
0.0416	1018.22	−0.1357	4.15	4.85
0.0576	1025.00	−0.1828	4.48	9.23
0.0969	1041.45	−0.3387	5.33	33.25
0.1390	1055.94	−0.4985	6.08	54.17
0.2018	1072.68	−0.7139	6.76	56.77
0.2844	1086.21	−0.8924	7.57	71.69
0.3649	1093.47	−0.9693	7.94	59.43
0.5110	1098.42	−0.9203	8.36	34.87
0.6791	1098.50	−0.6783	8.69	15.88
1.0000	1095.26	0.0000	9.17	0.00
		303.15 K		
0.0000	995.63	0.0000	3.23	0.00
0.0416	1016.27	−0.1352	4.15	4.40
0.0576	1022.85	−0.1818	4.48	8.68
0.0969	1038.78	−0.3348	5.34	32.64
0.1390	1052.82	−0.4922	6.10	53.60
0.2018	1069.03	−0.7047	6.79	56.27
0.2844	1082.11	−0.8817	7.60	71.35
0.3649	1089.17	−0.9612	7.98	59.09
0.5110	1093.86	−0.9158	8.39	34.56
0.6791	1093.73	−0.6761	8.73	15.67
1.0000	1090.24	0.0000	9.21	0.00
		308.15 K		
0.0000	994.01	0.0000	3.24	0.00
0.0416	1014.16	−0.1353	4.16	3.97
0.0576	1020.56	−0.1816	4.50	8.15
0.0969	1036.01	−0.3322	5.36	32.05
0.1390	1049.61	−0.4871	6.12	53.05
0.2018	1065.32	−0.6970	6.81	55.78
0.2844	1078.01	−0.8737	7.63	71.00
0.3649	1084.83	−0.9543	8.01	58.78
0.5110	1089.27	−0.9120	8.43	34.28
0.6791	1088.97	−0.6757	8.77	15.45
1.0000	1085.22	0.0000	9.25	0.00
		313.15 K		
0.0000	992.20	0.0000	3.24	0.00
0.0416	1011.88	−0.1353	4.17	3.56
0.0576	1018.12	−0.1816	4.51	7.65
0.0969	1033.12	−0.3300	5.37	31.50
0.1390	1046.33	−0.4832	6.14	52.53
0.2018	1061.55	−0.6902	6.83	55.33
0.2844	1073.88	−0.8670	7.66	70.68
0.3649	1080.46	−0.9481	8.04	58.50
0.5110	1084.67	−0.9089	8.46	34.02
0.6791	1084.18	−0.6742	8.81	15.27
1.0000	1080.21	0.0000	9.29	0.00
		318.15 K		
0.0000	990.17	0.0000	3.25	0.00
0.0416	1009.45	−0.1361	4.18	3.16
0.0576	1015.53	−0.1822	4.52	7.17
0.0969	1030.12	−0.3290	5.39	30.97
0.1390	1042.94	−0.4801	6.16	52.05
0.2018	1057.71	−0.6848	6.86	54.92
0.2844	1069.7	−0.8616	7.69	70.39
0.3649	1076.03	−0.9423	8.07	58.26
0.5110	1080.01	−0.9052	8.50	33.81
0.6791	1079.38	−0.6733	8.84	15.09
1.0000	1075.21	0.0000	9.34	0.00

[a]Standard uncertainties: $u(x) = 1 \times 10^{-4}$, $u(\rho) = 0.001$ kg·m^{-3}, $u(V_m^E) = 0.005 \times 10^{-6}$ m^3·mol^{-1}, $u(\alpha_p) = 0.05 \times 10^{-4}$ K^{-1}, $u(T) = 0.5$ K, $u(p) = 10$ kPa.

to 0.7 mol, nature (sharpness) and shift became more pronounced, which indicates interactions between S═O and H_2O as seen in Figure 4b. The H−O−H bending vibration peak broadening at 1650 cm^{-1} further confirms the involvement of water in the interactions with DMSO. The broadening of the O−H stretching vibration of water between 3200 and 3650 cm^{-1} is an indication of interaction due to H-bonding.

Spatial accommodation also plays a significant role in promoting strong bonding between DMSO and water molecules. DMSO acts as a hydrogen bond acceptor through its oxygen atom, forming stable hydrogen-bonded complexes with water molecules. In these complexes, water molecules interact with both the sulfoxide (S═O) group and the methyl groups of DMSO. These interactions contribute to the observed negative excess molar volume of the mixture.

Various researchers[44,45] have proposed that the properties exhibited by the DMSO + water system are consistent with the formation of polymeric species of the type—(DMSO·2H_2O). The extrema were observed at a mole fraction of approximately 0.33 for DMSO (corresponding to a DMSO:water ratio of 1:2) which lends support to this hypothesis. While the precise structure of these polymeric species cannot be determined from the current data, they are likely stabilized by hydrogen bonds between water molecules and the lone electron pairs on the oxygen atom of the sulfoxide group. These strong hydrogen-bonding interactions contribute to the observed negative excess molar volume as tighter molecular packing occurs within the mixture.

3.2. NMP + Water Binary Mixtures. For the binary mixtures of NMP + water, the trend is similar to that of DMSO + water given in Table 4. The density of the mixture increases

https://doi.org/10.1021/acs.jced.5c00049
J. Chem. Eng. Data XXXX, XXX, XXX−XXX

Table 4. Density (ρ), Excess Molar Volume (V_m^E), Coefficient of Thermal Expansion (α_p), and Excess of Coefficient of Thermal Expansion (α_p^E) as a Function of the Mole Fraction of NMP (x_1) at the Temperatures, T/K = (293.15−318.15) and Pressure, p = 0.1 MPa[a]

NMP (1) + water (2)				
x_1	ρ (kg·m^{-3})	V_m^E (10^{-6} m^3·mol^{-1})	α_p (10^{-4} K^{-1})	α_p^E (10^{-5} K^{-1})
293.15 K				
0.0000	998.21	0.0000	3.23	0.00
0.1575	1041.23	−0.7570	7.79	18.64
0.2209	1048.47	−0.9997	8.53	20.53
0.2608	1050.75	−1.1052	8.78	20.27
0.3025	1051.85	−1.1800	8.93	19.31
0.4290	1050.43	−1.2205	9.02	14.65
0.5148	1047.77	−1.1407	8.96	11.37
0.6242	1043.73	−0.9484	8.88	7.87
0.7713	1038.06	−0.5644	8.40	0.52
0.8763	1035.53	−0.3372	8.69	1.93
1.0000	1032.37	0.0000	8.64	0.00
298.15 K				
0.0000	997.04	0.0000	3.23	0.00
0.1575	1037.26	−0.7276	7.82	18.68
0.2209	1044.05	−0.9638	8.57	20.61
0.2608	1046.17	−1.0668	8.82	20.36
0.3025	1047.18	−1.1412	8.97	19.40
0.4290	1045.72	−1.1860	9.06	14.72
0.5148	1043.1	−1.1115	9.00	11.42
0.6242	1039.09	−0.9242	8.92	7.91
0.7713	1033.67	−0.5629	8.44	0.51
0.8763	1031.01	−0.3302	8.73	1.94
1.0000	1027.88	0.0000	8.68	0.00
303.15 K				
0.0000	995.63	0.0000	3.23	0.00
0.1575	1033.25	−0.7001	7.85	18.73
0.2209	1039.61	−0.9292	8.61	20.69
0.2608	1041.58	−1.0301	8.86	20.45
0.3025	1042.52	−1.1040	9.01	19.49
0.4290	1041.00	−1.1518	9.10	14.80
0.5148	1038.43	−1.0821	9.04	11.48
0.6242	1034.47	−0.9006	8.96	7.95
0.7713	1029.82	−0.6012	8.47	0.46
0.8763	1026.51	−0.3220	8.77	1.95
1.0000	1023.43	0.0000	8.71	0.00
308.15 K				
0.0000	994.01	0.0000	3.24	0.00
0.1575	1029.20	−0.6744	7.88	18.79
0.2209	1035.15	−0.8971	8.64	20.77
0.2608	1036.97	−0.9954	8.90	20.54
0.3025	1037.82	−1.0681	9.05	19.58
0.4290	1036.27	−1.1186	9.14	14.87
0.5148	1033.75	−1.0541	9.08	11.54
0.6242	1029.86	−0.8790	9.00	7.99
0.7713	1025.29	−0.5890	8.51	0.46
0.8763	1022.02	−0.3159	8.81	1.96
1.0000	1018.97	0.0000	8.75	0.00
313.15 K				
0.0000	992.20	0.0000	3.24	0.00
0.1575	1025.11	−0.6503	7.91	18.85
0.2209	1030.64	−0.8654	8.68	20.86
0.2608	1032.34	−0.9620	8.94	20.63
0.3025	1033.11	−1.0335	9.09	19.68
0.4290	1031.52	−1.0863	9.19	14.95
0.5148	1029.02	−1.0247	9.12	11.60
0.6242	1025.21	−0.8563	9.04	8.03
0.7713	1020.75	−0.5769	8.55	0.46
0.8763	1017.52	−0.3092	8.85	1.97
1.0000	1014.51	0.0000	8.79	0.00
318.15 K				
0.0000	990.17	0.0000	3.25	0.00
0.1575	1020.95	−0.6269	7.94	18.91
0.2209	1026.09	−0.8348	8.72	20.96
0.2608	1027.67	−0.9290	8.98	20.73
0.3025	1028.35	−0.9990	9.14	19.78
0.4290	1026.73	−1.0533	9.23	15.03
0.5148	1024.29	−0.9954	9.17	11.67
0.6242	1020.56	−0.8333	9.08	8.08
0.7713	1016.18	−0.5617	8.59	0.47
0.8763	1013.02	−0.3012	8.88	1.98
1.0000	1010.07	0.0000	8.83	0.00

[a]Standard uncertainties $u(x) = 1 \times 10^{-4}$, $u(\rho) = 0.001$ kg·m^{-3}, $u(V_m^E) = 0.005 \times 10^{-6}$ m^3·mol^{-1}, $u(\alpha_p) = 0.05 \times 10^{-4}$ K^{-1}, $u(T) = 0.5$ K, $u(p) = 10$ kPa.

with an increase in x_1, the mole fraction of NMP, at all temperatures (293.15−318.15 K), while the density decreases gradually as the temperature rises. Like the DMSO + water mixture, the NMP + water mixtures also exhibit negative excess molar volume (V_m^E) within the mole fraction range of 0.3 to 0.4 as seen in Figure 5. The excess coefficient of thermal expansion (α_p^E) also shows positive values with an increase in concentration of NMP and temperature as seen in Figure 6. The trends in both properties indicate the presence of strong intermolecular interactions within the NMP + water solution.

NMP, a polar aprotic solvent with a strong solubilizing ability, interacts with water molecules primarily through hydrogen bonding.[46] The oxygen atom in the NMP structure acts as a hydrogen bond acceptor, disrupting water's hydrogen-bonding network while simultaneously forming hydrogen bonds with water molecules. These interactions led to the formation of stable hydrogen-bonded complexes within the mixture. Research has shown that the C═O bond in NMP elongates in the presence of water, which enhances the hydrogen-bonding capability of the mixture. The excess molar volume is sensitive to molecular interactions and packing factor.[47] The study by Basma et al.[48] shows that relative to other aromatic and aliphatic solvents, NMP has denser intermolecular packing, significantly more long-range molecular organization, and a greater range of local interactions. Various researchers[47,49,50] suggest a formation of polymeric molecules between two water molecules and one NMP molecule via the two lone pairs of electrons on the oxygen atom of a carbonyl group. The excess molar volume has been studied by Zaichikov[51] and shows negative V_m^E values representing the different structural organizations in an aqueous NMP solution. For lower concentrations of NMP,

https://doi.org/10.1021/acs.jced.5c00049
J. Chem. Eng. Data XXXX, XXX, XXX−XXX

Table 5. Density (ρ), Excess Molar Volume (V_m^E), Coefficient of Thermal Expansion (α_p), and Excess of Coefficient of Thermal Expansion (α_p^E) as a Function of the Mole Fraction of DMSO (x_1) at the Temperatures, T/K = (293.15−318.15) and Pressure, P = 0.1 MPa[a]

DMSO (1) + NMP (2)				
x_1	ρ (kg·m^{-3})	V_m^E (10^{-6} m^3·mol^{-1})	α_p (10^{-4} K^{-1})	α_p^E (10^{-6} K^{-1})
		293.15 K		
0.0000	1032.37	0.0000	−8.64	0.00
0.2616	1046.46	0.0101	−8.74	−6.13
0.3667	1052.49	0.0286	−8.79	−5.70
0.4745	1059.09	0.0449	−8.86	−3.43
0.5739	1065.76	0.0443	−8.90	1.90
0.6699	1072.62	0.0425	−8.96	4.92
0.7588	1079.36	0.0404	−8.99	7.47
0.8431	1086.33	0.0239	−9.05	5.18
0.9232	1093.25	0.0134	−9.09	2.81
1.0000	1100.31	0.0000	−9.12	0.00
		298.15 K		
0.0000	1027.88	0.0000	−8.68	0.00
0.2616	1041.86	0.0104	−8.78	−6.18
0.3667	1047.83	0.0298	−8.83	−5.76
0.4745	1054.39	0.0449	−8.90	−3.45
0.5739	1060.98	0.0463	−8.94	1.91
0.6699	1067.81	0.0426	−9.00	4.98
0.7588	1074.48	0.0415	−9.03	7.54
0.8431	1081.41	0.0234	−9.09	5.25
0.9232	1088.24	0.0150	−9.13	2.82
1.0000	1095.26	0.0000	−9.17	0.00
		303.15 K		
0.0000	1023.43	0.0000	−8.72	0.00
0.2616	1037.30	0.0090	−8.82	−6.22
0.3667	1043.20	0.0302	−8.87	−5.80
0.4745	1049.69	0.0467	−8.94	−3.48
0.5739	1056.26	0.0455	−8.98	1.96
0.6699	1063.01	0.0435	−9.04	5.03
0.7588	1069.63	0.0417	−9.07	7.62
0.8431	1076.49	0.0244	−9.13	5.30
0.9232	1083.26	0.0164	−9.18	2.84
1.0000	1090.24	0.0000	−9.21	0.00
		308.15 K		
0.0000	1018.97	0.0000	−8.75	0.00
0.2616	1032.73	0.0092	−8.86	−6.28
0.3667	1038.57	0.0313	−8.91	−5.86
0.4745	1045.00	0.0481	−8.98	−3.51
0.5739	1051.52	0.0461	−9.02	1.98
0.6699	1058.20	0.0451	−9.08	5.08
0.7588	1064.77	0.0430	−9.11	7.68
0.8431	1071.57	0.0256	−9.18	5.35
0.9232	1078.30	0.0162	−9.22	2.88
1.0000	1085.22	0.0000	−9.25	0.00
		313.15 K		
0.0000	1014.51	0.0000	−8.79	0.00
0.2616	1028.15	0.0106	−8.90	−6.34
0.3667	1033.97	0.0302	−8.95	−5.89
0.4745	1040.32	0.0492	−9.02	−3.53
0.5739	1046.77	0.0485	−9.06	1.99
0.6699	1053.41	0.0461	−9.12	5.13
0.7588	1059.93	0.0436	−9.16	7.76
0.8431	1066.66	0.0271	−9.22	5.39
0.9232	1073.35	0.0167	−9.26	2.91
1.0000	1080.21	0.0000	−9.29	0.00
		318.15 K		
0.0000	1010.07	0.0000	−8.83	0.00
0.2616	1023.58	0.0109	−8.94	−6.40
0.3667	1029.34	0.0315	−8.99	−5.95
0.4745	1035.64	0.0504	−9.06	−3.56
0.5739	1042.04	0.0493	−9.10	2.02
0.6699	1048.6	0.0485	−9.16	5.17
0.7588	1055.1	0.0438	−9.20	7.84
0.8431	1061.75	0.0287	−9.26	5.44
0.9232	1068.39	0.0173	−9.30	2.94
1.0000	1075.21	0.0000	−9.34	0.00

[a]Standard uncertainties $u(x)$ = 1 × 10^{-4}, $u(\rho)$ = 0.001 kg·m^{-3}, $u(V_m^E)$ = 0.005 × 10^{-6}m^3·mol^{-1}, $u(\alpha_p)$ = 0.05 × 10^{-4} K^{-1}, $u(T)$ = 0.5 K, $u(p)$ = 10 kPa.

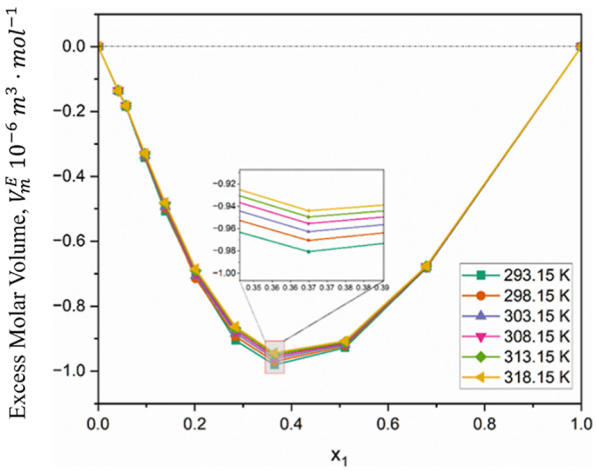

Figure 2. Excess molar volume (V_m^E) of DMSO (1) + water (2) liquid mixtures at various temperatures as a function of x_1.

the solution experiences trivial structural changes, a hetero-association of $C_5H_9NO{\cdot}2H_2O$, and hydrophobic interactions between amide molecules. The study further reports breakage of the hydrogen-bonding network of water and a maximum hetero-association between 0.33 < x_1 < 0.35 where more negative V_m^E values are seen.[51] The DFT study carried out by Aparicio et al.[36] also reveals the efficient packing of NMP molecules in a water hydrogen-bonding network and favorable hetero-association in a 1:2 NMP:water ratio around a 0.3 mole fraction. The literature[32,36,47,50,51] strengthens our current observation about NMP + water showing negative V_m^E values at all temperatures hence indicating strong intermolecular forces and tighter molecular packing. The intermolecular interactions are further analyzed with FTIR at two different concentrations (x_1 = 0.2 and 0.9) of NMP.

The solution showing the FTIR spectra in Figure 7a has a lower concentration of NMP (x_1 = 0.2). The broadening of water's O−H stretching vibration (3200−3650 cm^{-1}) in the NMP−water mixture and shift in the NMP C═O peak

https://doi.org/10.1021/acs.jced.5c00049
J. Chem. Eng. Data XXXX, XXX, XXX−XXX

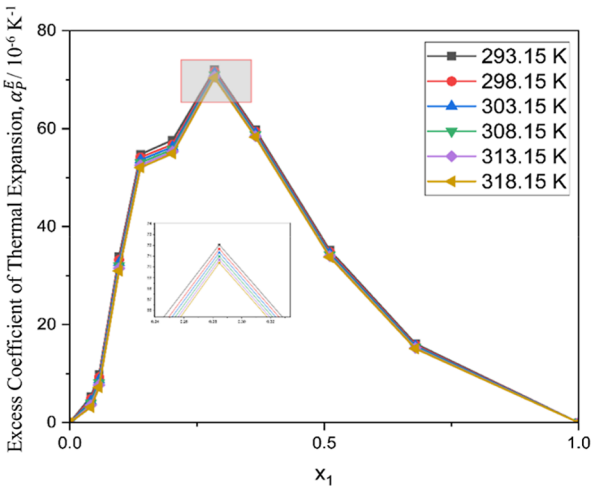

Figure 3. Excess coefficient of thermal expansion (α_P^E) of DMSO (1) + water (2) liquid mixtures at various temperatures as a function of x_1.

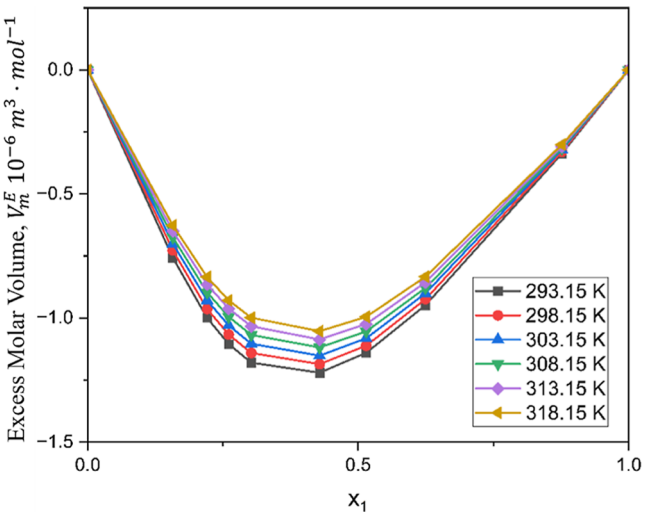

Figure 5. Excess molar volume (V_m^E) of NMP (1) + water (2) liquid mixtures at various temperatures as a function of x_1.

(1660−1700 cm^{-1}) are indicative of interactions between the constituents. Further, the change in the nature of the peak of the C−H stretch (2800−3000 cm^{-1}) in NMP + water demonstrates the possible interaction of NMP−water. In Figure 7b, as the concentration of NMP increased (x_1 = 0.9) and the water concentration reduced significantly from 0.8 to 0.1 mol, almost all interactions diminished OR significantly reduced. Hence, in the NMP + water mixture, it is very hard to see the broad O−H stretching vibration (3200−3650 cm^{-1}) of water and the reappearance of the C−H stretch-aliphatic spectra (2800−300 cm^{-1}). Also, there is hardly any shift in the NMP C═O peak (1660−1700 cm^{-1}) when the water concentration was reduced from 0.8 to 0.1 mol.

As seen from Table 2, the densities of pure NMP and DMSO have minor differences at all temperatures. It is observed from the evaluation of thermophysical properties that their intermolecular behavior or interactions with water are similar (Tables 3 and 4). The extrema in the V_m^E value are seen between a mole fraction range of 0.3 and 0.4 for both mixtures; however, the values were more negative for NMP + water mixtures than DMSO + water mixtures. This indicates molar volume occupied by NMP + water molecules is higher than expected, hence depicting stronger intermolecular interactions than DMSO + water molecules.[47] The higher V_m^E values also resulted from the efficient packing factor of NMP + water molecules.[47]

3.3. DMSO + NMP Binary Mixtures. For the binary mixtures of DMSO + NMP, the density increases with increasing x_1, the mole fraction of DMSO, at all temperatures (293.15 to 318.15 K) as seen in Table 5. Conversely, the density decreases with rising temperatures across all compositions, consistent with typical thermal expansion behavior. In contrast to the DMSO + water and NMP + water systems, the excess molar volume for the DMSO + NMP mixtures is positive over the entire range of compositions, as shown in Figure 8. The positive values of V_m^E can be attributed to dispersion forces and the destruction of self-associated

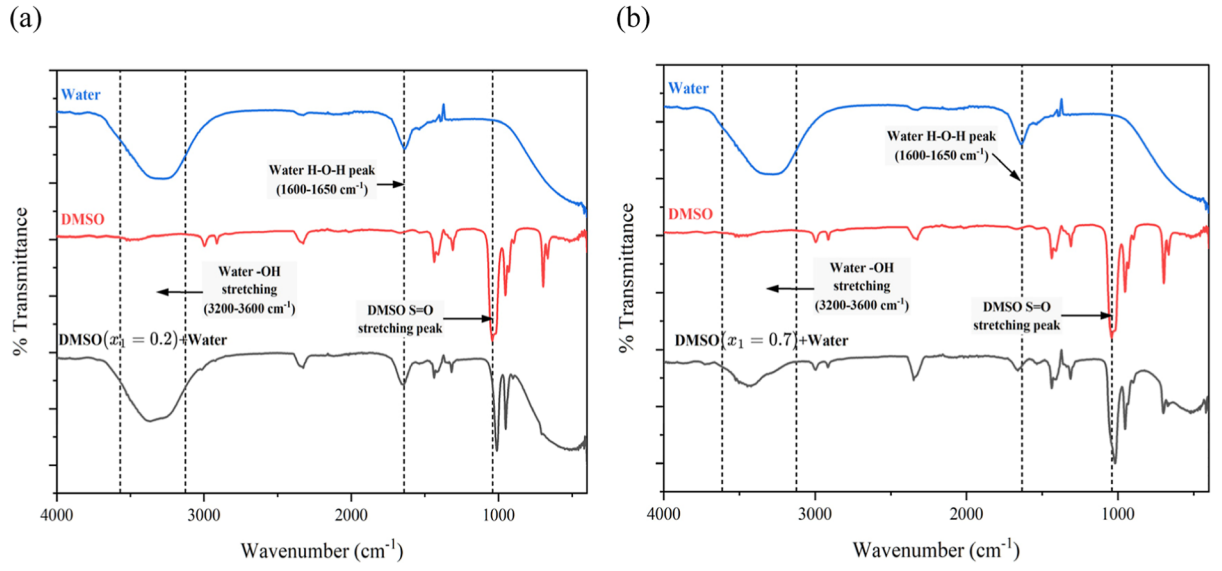

Figure 4. (a) FTIR spectra of a binary mixture of DMSO (1) (x_1 = 0.2) + water (2); (b) FTIR spectra of a binary mixture of DMSO (1) (x_1 = 0.7) + water (2).

https://doi.org/10.1021/acs.jced.5c00049
J. Chem. Eng. Data XXXX, XXX, XXX−XXX

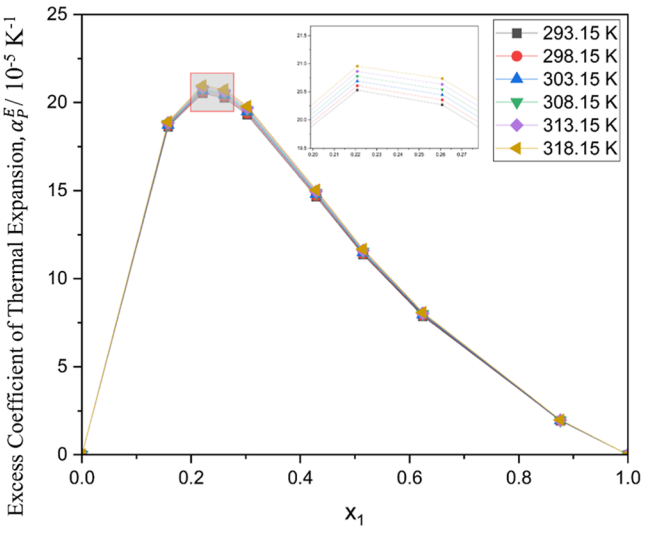

Figure 6. Excess coefficient of thermal expansion (α_P^E) of NMP (1) + water (2) liquid mixtures at various temperatures as a function of x_1.

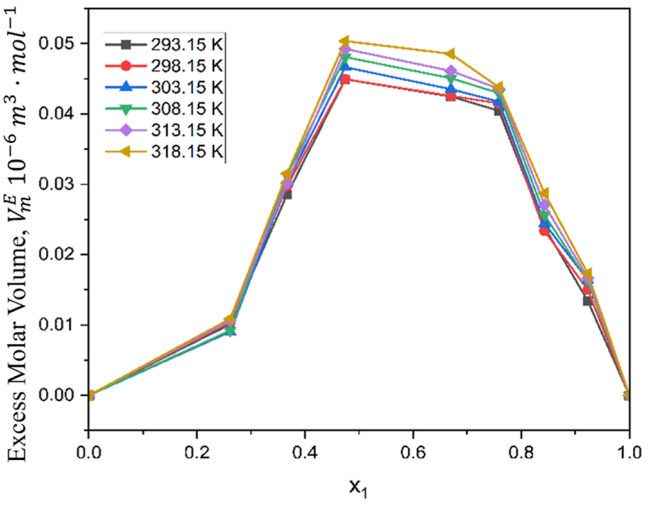

Figure 8. Excess molar volume (V_m^E) of DMSO (1) + NMP (2) liquid mixtures at various temperatures as a function of x_1.

complexes in pure liquids.[52] The excess of the coefficient of thermal expansion shows interesting trends for DMSO and NMP solutions as seen in Figure 9. The negative α_P^E values are seen between a 0.2 and 0.3 mole fraction range for lower concentrations of DMSO wherein positive α_P^E values are seen between 0.7 and 0.8 mole fractions for higher concentrations of DMSO for all the temperatures. This may have occurred due to self-association and tight molecular packing of pure liquids.

Both DMSO and NMP are highly polar molecules that exhibit significant self-association in their pure states. When mixed, the destruction of these self-associated complexes leads to the formation of a less tightly packed binary solution, resulting in positive excess molar volumes. Furthermore, the positive values of V_m^E increase with temperature, which can be attributed to the expansion of the free volume within the mixture.[53] The intermolecular interactions in DMSO + NMP mixtures are primarily governed by dipole−dipole and dispersion forces rather than hydrogen bonding. The complementary polarities and electronic structures of DMSO and NMP promote interactions that disrupt self-association, contributing to the observed behavior.

The FTIR spectra show the presence of interactions within the solution. The DMSO at 0.9 and NMP at 0.1 mole fraction interactions are indistinguishable as the DMSO + NMP mixture peaks are mirroring pure DMSO as seen in Figure 10b. But, as the concentration of NMP was increased from 0.1 to 0.3 mole fraction, a change in the nature of the S═O peak of DMSO (1050 cm^{-1}) from a broad peak in DMSO to a sharp peak in the DMSO−NMP mixture is seen in Figure 10b, indicative of dipole−dipole interaction of DMSO S═O and NMP C═O.

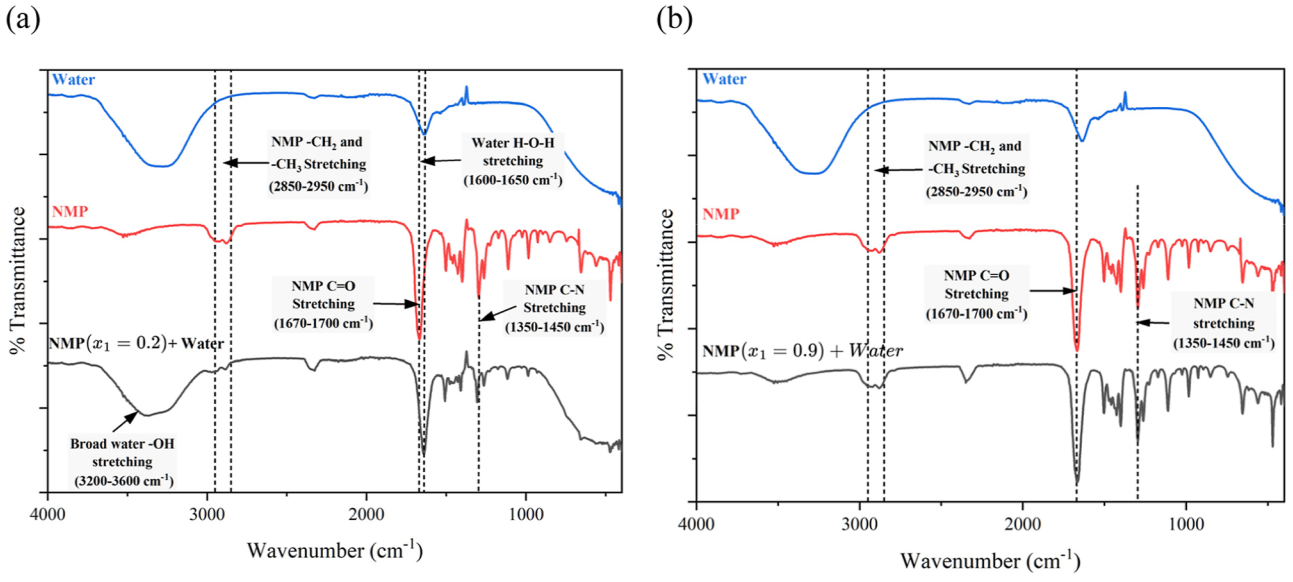

Figure 7. (a) FTIR spectra of binary mixtures of NMP (1) (x_1 = 0.2) + water (2); (b) FTIR spectra of binary mixtures of NMP (1) (x_1 = 0.9) + water (2).

https://doi.org/10.1021/acs.jced.5c00049
J. Chem. Eng. Data XXXX, XXX, XXX−XXX

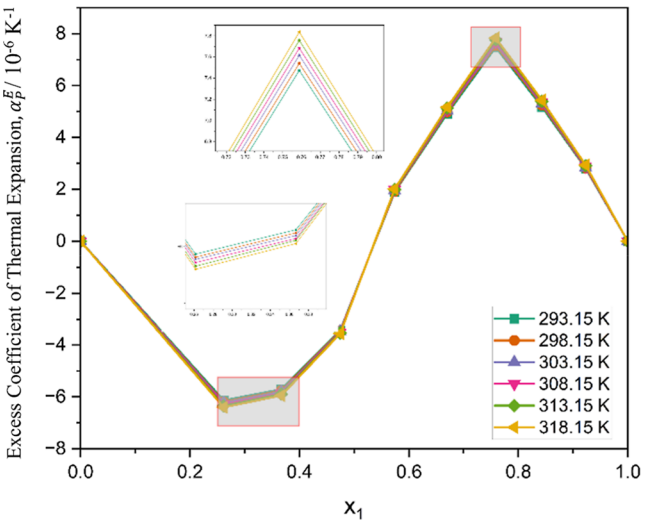

Figure 9. Excess coefficient of thermal expansion (α_P^E) of DMSO (1) + NMP (2) liquid mixtures at various temperatures as a function of x_1.

4. CONCLUSIONS

The combined study of thermophysical properties and FTIR analysis for the binary mixtures of DMSO + water, NMP + water, and DMSO + NMP has provided a comprehensive understanding of the molecular interactions and structural behavior of these systems.

For DMSO + water and NMP + water mixtures, the extrema in excess molar volume and FTIR spectral shifts support the formation of stable hydrogen-bonded polymeric species. The FTIR results confirm the disruption of the water hydrogen-bonding network and the formation of new hydrogen bonds with DMSO and NMP molecules. In contrast, the DMSO + NMP mixtures exhibit positive excess molar volumes across all compositions. FTIR analysis reveals weak dipole−dipole interactions and the breaking of self-associated complexes in the pure liquids, resulting in positive V_m^E values that increase with temperature.

These findings demonstrate the utility of combining thermophysical property measurements with FTIR spectroscopy to elucidate molecular interactions. The results not only advance the fundamental understanding of these mixtures but also have practical implications for optimizing solvent systems in chemical processes, separation technologies, and environmental applications. Future work could include molecular dynamics simulations and advanced spectroscopic techniques to further explore the dynamic behavior and structural organization of these systems.

■ ASSOCIATED CONTENT

Supporting Information

The Supporting Information is available free of charge at https://pubs.acs.org/doi/10.1021/acs.jced.5c00049.

Comparison plots of measured density with literature values of pure components and comparative plots of density with literature values of similar binary mixtures (PDF)

■ AUTHOR INFORMATION

Corresponding Author

Ranjan Dey − *Thermophysical Properties Lab, Department of Chemistry, Birla Institute of Technology and Science, Sancoale, Goa 403726, India;* orcid.org/0000-0001-8914-8519; Email: ranjandey@goa.bits-pilani.ac.in

Authors

Praseeda P. Nair − *Thermophysical Properties Lab, Department of Chemistry, Birla Institute of Technology and Science, Sancoale, Goa 403726, India*

Aditi Prabhune − *Thermophysical Properties Lab, Department of Chemistry, Birla Institute of Technology and Science, Sancoale, Goa 403726, India;* orcid.org/0000-0003-4899-3825

Sanjay Kumar − *Thermophysical Properties Lab, Department of Chemistry, Birla Institute of Technology and Science, Sancoale, Goa 403726, India;* orcid.org/0009-0002-5574-5547

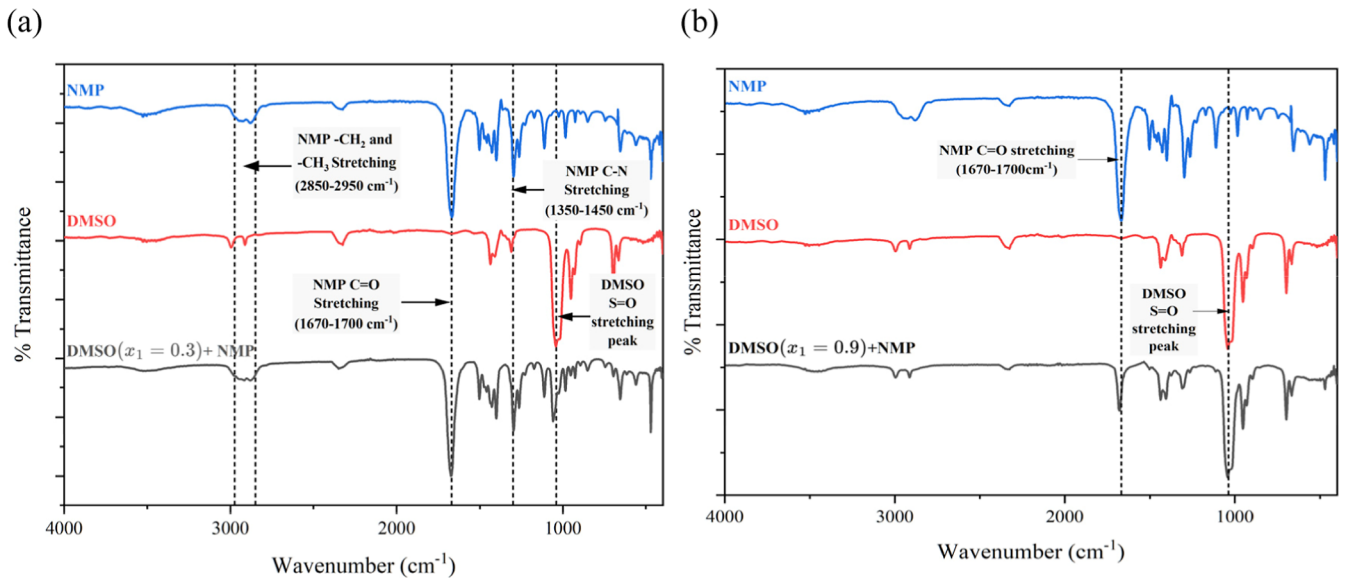

Figure 10. (a) FTIR spectra of binary mixtures of DMSO (1) (x_1 = 0.3) + NMP (2); (b) FTIR spectra of binary mixtures of DMSO (1) (x_1 = 0.9) + NMP (2).

https://doi.org/10.1021/acs.jced.5c00049
J. Chem. Eng. Data XXXX, XXX, XXX−XXX

Complete contact information is available at:
https://pubs.acs.org/10.1021/acs.jced.5c00049

Author Contributions

Ranjan Dey conceived and designed the study. Praseeda P Nair and Aditi Prabhune performed the experiments, collected the data, and carried out the data analysis. Sanjay Kumar contributed to the FTIR analysis and interpretation. All authors contributed to the discussion of results and preparation of the manuscript and approved the final version for submission.

Notes

The authors declare no competing financial interest.

■ ACKNOWLEDGMENTS

Authors Praseeda P Nair and Ranjan Dey acknowledge the financial assistance from the CDRF Project Grant C1/23/152 from BITS Pilani, University.

■ REFERENCES

(1) Reichardt, C.; Welton, T. *Solvents and Solvent Effects in Organic Chemistry*; Wiley VCH, 2011.
(2) Buncel, E.; Stairs, R. A.; Wilson, H. *The Role of the Solvent in Chemical Reactions*; Oxford University Press Oxford, 2003.
(3) Giudicessi, S. L.; Saavedra, S. L.; Cardillo, A. B.; Camperi, S. A.; Cascone, O.; Albericio, F.; Martínez Ceron, M. C. Chapter 5—Green Solvents in the Biotechnology-Based Pharmaceutical Industry. In *Green Sustainable Process for Chemical and Environmental Engineering and Science*; Elsevier, 2021; pp 87−104..
(4) Solvents Use in Various Industries*Handbook of Solvents*; Wypych, G., Ed.; Elsevier, 2019; pp 901−1124..
(5) Prabhune, A.; Dey, R. Green and Sustainable Solvents of the Future: Deep Eutectic Solvents. *J. Mol. Liq.* **2023**, *379*, 121676.
(6) Halios, C. H.; Landeg-Cox, C.; Lowther, S. D.; Middleton, A.; Marczylo, T.; Dimitroulopoulou, S. Chemicals in European Residences − Part I: A Review of Emissions, Concentrations and Health Effects of Volatile Organic Compounds (VOCs). *Sci. Total Environ.* **2022**, *839*, 156201.
(7) Li, A. J.; Pal, V. K.; Kannan, K. A Review of Environmental Occurrence, Toxicity, Biotransformation and Biomonitoring of Volatile Organic Compounds. *Environ. Chem. Ecotoxicol.* **2021**, *3*, 91−116.
(8) Winterton, N. The Green Solvent: A Critical Perspective. *Clean Technol. Environ. Policy* **2021**, *23* (9), 2499−2522.
(9) Parker, A. J. The Effects of Solvation on the Properties of Anions in Dipolar Aprotic Solvents. *Q. Rev., Chem. Soc.* **1962**, *16* (2), 163.
(10) Di Mino, C.; Clancy, A. J.; Sella, A.; Howard, C. A.; Headen, T. F.; Seel, A. G.; Skipper, N. T. Weak Interactions in Dimethyl Sulfoxide (DMSO)−Tertiary Amide Solutions: The Versatility of DMSO as a Solvent. *J. Phys. Chem. B* **2023**, *127* (6), 1357−1366.
(11) Wu, X.-F. *Solvents as Reagents in Organic Synthesis: Reactions and Applications*; John Wiley & Sons, 2018.
(12) Åkesson, B.; Jönsson, B. A. Biological Monitoring of N-Methyl-2-Pyrrolidone Using 5-Hydroxy-N-Methyl-2-Pyrrolidone in Plasma and Urine as the Biomarker. *Scand. J. Work, Environ. Health* **2000**, *26* (3), 213−218.
(13) Wang, H.; Xie, K.; Wang, L.; Han, Y. N-Methyl-2-Pyrrolidone as a Solvent for the Non-Aqueous Electrolyte of Rechargeable Li-Air Batteries. *J. Power Sources* **2012**, *219*, 263−271.
(14) Jouyban, A.; Fakhree, M. A. A.; Shayanfar, A. Review of Pharmaceutical Applications of N-Methyl-2-Pyrrolidone. *J. Pharm. Pharm. Sci.* **2010**, *13* (4), 524.
(15) Dey, R.; Prabhune, A. Ultrasonic, Surface Tension and Thermoacoustical Studies of Alkanone + Amine Mixtures. *Chem. Pap.* **2024**, *78* (16), 8863−8876.
(16) Arokiaraj, R. G.; Raju, R.; Ravikumar, S.; Sivakumar, K.; Bhanuprakash, P.; Pandiyan, V. Excess Thermodynamic Properties and FTIR Studies of Binary Mixtures of Aniline with Esters at Different Temperatures. *Chem. Data Collect.* **2022**, *37*, 100807.
(17) Sekhar Pattanaik, S.; Nanda, B.; Ranjan Panda, S.; Dalai, B.; Nanda, B. B. Investigation of the Inter-Ionic Interactions of an Imidazolium-Based Ionic Liquid with the Aqueous Solutions of Tripotassium Citrate and Trisodium Citrate through Volumetric, Acoustic and FTIR Routes. *J. Mol. Liq.* **2022**, *351*, 118644.
(18) Ganji, S.; Krishna, T. S.; Venkatesan, D.; Day, R.; Ramachandran, D. Thermodynamic and Transport Properties of Binary Mixtures Containing 1,2-Propanediol with 2-Methoxyethanol and 2-Ethoxyethanol at Different Temperatures. *J. Chem. Thermodyn.* **2025**, *201*, 107396.
(19) Rama Rao, P. V. S. S.; Krishna, T. S.; Bharath, P.; Dey, R.; Ramachandran, D. Understanding of Molecular Interactions between Ethyl Acetate and 1-Butyl-3-Methyl-Imidazolium Bis-(Trifluoromethylsulfonyl)Imide: A Thermophysical Study. *J. Chem. Thermodyn.* **2021**, *156*, 106383.
(20) Oswal, S. L.; Pandiyan, V.; Krishnakumar, B.; Vasantharani, P. Thermodynamic and Acoustic Properties of Binary Mixtures of Oxolane with Aniline and Substituted Anilines at 303.15, 313.15 and 323.15K. *Thermochim. Acta* **2010**, *507*−*508*, 27−34.
(21) Haynes, W. *CRC Handbook of Chemistry and Physics*, 94th ed.; Haynes, W. M., Lide, D. R., Eds.; CRC Press, 2013.
(22) Zarei, H. A.; Lavasani, M. Z.; Iloukhani, H. Densities and Volumetric Properties of Binary and Ternary Liquid Mixtures of Water (1) + Acetonitrile (2) + Dimethyl Sulfoxide (3) at Temperatures from (293.15 to 333.15) K and at Ambient Pressure (81.5 KPa). *J. Chem. Eng. Data* **2008**, *53* (2), 578−585.
(23) Liu, J.; Zhu, C.; Ma, Y. Densities and Viscosities of Binary Solutions of Benzene-1,3-Diol + Water, Ethanol, Propan-1-Ol, and Butan-1-Ol at T = (293.15 to 333.15) K. *J. Chem. Eng. Data* **2011**, *56* (5), 2095−2099.
(24) Zhuchkov, V.; Raeva, V.; Frolkova, A. Densities and Excess Volumes of Binary and Ternary Mixtures of N, N-Dimethyl Sulfoxide, N,N-Dimethylacetamide, and N-Methyl-2-Pyrrolidone at T = (293.15, 313.15)K and Atmospheric Pressure. *Chem. Data Collect.* **2022**, *38*, 100840.
(25) Agieienko, V.; Buchner, R. A Comprehensive Study of Density, Viscosity, and Electrical Conductivity of (Choline Chloride + Glycerol) Deep Eutectic Solvent and Its Mixtures with Dimethyl Sulfoxide. *J. Chem. Eng. Data* **2021**, *66* (1), 780−792.
(26) Iulian, O.; Ciocirlan, O. Volumetric Properties of Binary Mixtures of Two 1-Alkyl-3-Methylimidazolium Tetrafluoroborate Ionic Liquids with Molecular Solvents. *J. Chem. Eng. Data* **2012**, *57* (10), 2640−2646.
(27) Murrieta-Guevara, F.; Trejo Rodriguez, A. Liquid Density as a Function of Temperature of Five Organic Solvents. *J. Chem. Eng. Data* **1984**, *29* (2), 204−206.
(28) Yao, H.; Zhang, S.; Wang, J.; Zhou, Q.; Dong, H.; Zhang, X. Densities and Viscosities of the Binary Mixtures of 1-Ethyl-3-Methylimidazolium Bis(Trifluoromethylsulfonyl)Imide with N -Methyl-2-Pyrrolidone or Ethanol at T = (293.15 to 323.15) K. *J. Chem. Eng. Data* **2012**, *57* (3), 875−881.
(29) Grande, M. d. C.; Juliá, J. A.; García, M.; Marschoff, C. M. On the Density and Viscosity of (Water + Dimethylsulfoxide) Binary Mixtures. *J. Chem. Thermodyn.* **2007**, *39* (7), 1049−1056.
(30) Ghazoyan, H. H.; Grigoryan, Z. L.; Gabrielyan, L. S.; Markarian, S. A. Study of Thermodynamic Properties of Binary Mixtures of Propionitrile with Dimethylsulfoxide (or Diethylsulfoxide) at Temperatures from (298.15 to 323.15)K. *J. Mol. Liq.* **2019**, *284*, 147−156.
(31) García-Giménez, P.; Gil, L.; Blanco, S. T.; Velasco, I.; Otín, S. Densities and Isothermal Compressibilities at Pressures up to 20 MPa of the Systems 1-Methyl-2-Pyrrolidone + 1-Chloroalkane or + α,ω-Dichloroalkane. *J. Chem. Eng. Data* **2008**, *53* (1), 66−72.
(32) Makarov, D. M.; Dyshin, A. A.; Krestyaninov, M. A.; Ivlev, D. V.; Kolker, A. M. Hydrogen Bonds in a Water−Pyrrolidone System. *Russ. J. Phys. Chem. A* **2022**, *96* (4), 685−690.

(33) George, J.; Sastry, N. V. Densities, Viscosities, Speeds of Sound, and Relative Permittivities for Water + Cyclic Amides (2-Pyrrolidinone, 1-Methyl-2-Pyrrolidinone, and 1-Vinyl-2-Pyrrolidinone) at Different Temperatures. *J. Chem. Eng. Data* **2004**, *49* (2), 235−242.
(34) Zarei, H. A.; Lavasani, M. Z.; Iloukhani, H. Densities and Volumetric Properties of Binary and Ternary Liquid Mixtures of Water (1) + Acetonitrile (2) + Dimethyl Sulfoxide (3) at Temperatures from (293.15 to 333.15) K and at Ambient Pressure (81.5 KPa). *J. Chem. Eng. Data* **2008**, *53* (2), 578−585.
(35) Tôrres, R. B.; Marchiore, A. C. M.; Volpe, P. L. O. Volumetric Properties of Binary Mixtures of (Water + Organic Solvents) at Temperatures between T = 288.15 K and T = 303.15 K at p = 0.1 MPa. *J. Chem. Thermodyn.* **2006**, *38* (5), 526−541.
(36) Aparicio, S.; Alcalde, R.; Dávila, M. J.; García, B.; Leal, J. M. Measurements and Predictive Models for the N-Methyl-2-Pyrrolidone/Water/Methanol System. *J. Phys. Chem. B* **2008**, *112* (36), 11361−11373.
(37) Verma, S.; Kim, S.; Maken, S.; Lee, Y. Thermodynamic and Molecular Simulation Analysis of Molecular Interactions between Methyl 2−Hydroxyisobutyrate + Water or n−Alkanol (C1−C2) Mixtures. *J. Mol. Liq.* **2023**, *392*, 123461.
(38) Prabhune, A.; Saini, A.; Dey, R. Physicochemical Behaviour of 2-Pentanone + Amine Mixtures at Three Temperatures. *J. Indian Chem. Soc.* **2023**, *100* (7), 101031.
(39) Nain, A. K. Study of Intermolecular Interactions in Binary Mixtures of Methyl Acrylate with Benzene and Methyl Substituted Benzenes at Different Temperatures: An Experimental and Theoretical Approach. *Chin. J. Chem. Eng.* **2022**, *44*, 212−238.
(40) Lebel, R. G.; Goring, D. A. I. Density, Viscosity, Refractive Index, and Hygroscopicity of Mixtures of Water and Dimethyl Sulfoxide. *J. Chem. Eng. Data* **1962**, *7* (1), 100−101.
(41) MacGregor, W. S. THE CHEMICAL AND PHYSICAL PROPERTIES OF DMSO. *Ann. N.Y. Acad. Sci.* **1967**, *141* (1), 3−12.
(42) Śmiechowski, M. The Influence of Intermolecular Correlations on the Infrared Spectrum of Liquid Dimethyl Sulfoxide. *Spectrochim. Acta, Part A* **2021**, *260*, 119869.
(43) Oh, K.; Rajesh, K.; Stanton, J. F.; Baiz, C. R. Quantifying Hydrogen-Bond Populations in Dimethyl Sulfoxide/Water Mixtures. *Angew. Chem., Int. Ed.* **2017**, *56* (38), 11375−11379.
(44) Luzar, A.; Chandler, D. Structure and Hydrogen Bond Dynamics of Water−Dimethyl Sulfoxide Mixtures by Computer Simulations. *J. Chem. Phys.* **1993**, *98* (10), 8160−8173.
(45) Roy, S.; Banerjee, S.; Biyani, N.; Jana, B.; Bagchi, B. Theoretical and Computational Analysis of Static and Dynamic Anomalies in Water−DMSO Binary Mixture at Low DMSO Concentrations. *J. Phys. Chem. B* **2011**, *115* (4), 685−692.
(46) Aparicio, S.; Alcalde, R.; Dávila, M. J.; García, B.; Leal, J. M. Measurements and Predictive Models for the *N* -Methyl-2-Pyrrolidone/Water/Methanol System. *J. Phys. Chem. B* **2008**, *112* (36), 11361−11373.
(47) MacDonald, D. D.; Dunay, D.; Hanlon, G.; Hyne, J. B. Properties of the N-Methyl-2-Pyrrolidinone-Water System. *Can. J. Chem. Eng.* **1971**, *49* (3), 420−423.
(48) Basma, N. S.; Headen, T. F.; Shaffer, M. S. P.; Skipper, N. T.; Howard, C. A. Local Structure and Polar Order in Liquid N-Methyl-2-Pyrrolidone (NMP). *J. Phys. Chem. B* **2018**, *122* (38), 8963−8971.
(49) García, B.; Alcalde, R.; Leal, J. M.; Matos, J. S. Solute−Solvent Interactions in Amide−Water Mixed Solvents. *J. Phys. Chem. B* **1997**, *101* (40), 7991−7997.
(50) Henni, A.; Hromek, J. J.; Tontiwachwuthikul, P.; Chakma, A. Volumetric Properties and Viscosities for Aqueous N-Methyl-2-Pyrrolidone Solutions from 25°C to 70°C. *J. Chem. Eng. Data* **2004**, *49* (2), 231−234.
(51) Zaichikov, A. M. Thermodynamic Characteristics of Water-N-Methylpyrrolidone Mixtures and Intermolecular Interactions in Them. *Russ. J. Gen. Chem.* **2006**, *76* (4), 626−633.
(52) Ramos-Estrada, M.; López-Cortés, I. Y.; Iglesias-Silva, G. A.; Pérez-Villaseñor, F. Density, Viscosity, and Speed of Sound of Pure and Binary Mixtures of Ionic Liquids Based on Sulfonium and Imidazolium Cations and Bis(Trifluoromethylsulfonyl)Imide Anion with 1-Propanol. *J. Chem. Eng. Data* **2018**, *63* (12), 4425.
(53) George, J.; Sastry, N. V.; Patel, S. R.; Valand, M. K. Densities, Viscosities, Speeds of Sound, and Relative Permittivities for Methyl Acrylate + 1-Alcohols ($C_1 - C_6$) at T = (308.15 and 318.15) K. *J. Chem. Eng. Data* **2002**, *47* (2), 262−269.

https://doi.org/10.1021/acs.jced.5c00049
J. Chem. Eng. Data XXXX, XXX, XXX−XXX